Effects of Disorder in Reduced Dimensional and Quantum Electronics

B.D. Weaver* and E.H. Aifer**
Naval Research Laboratory, Code 6818, 4555 Overlook Ave., SW, Washington, DC 20375
*weaver1@ccf.nrl.navy.mil
**aifer@estd.nrl.navy.mil

ABSTRACT

We discuss the effect of atomic disorder on electronic systems that operate in either reduced dimension or by quantum-mechanical transport. Systems include high electron mobility transistors, tunnel diodes, superconductors, multiquantum well infrared and ultraviolet detectors, and superlattice devices. In most cases, quantum mechanics and/or reduced dimension produces an unconventional response to disorder, rendering some devices more sensitive to disorder, and other devices more tolerant.

Keywords: nanoelectronics, radiation, HEMT, RTD.

1 INTRODUCTION

As the size and dimensionality of electronic devices is decreased, the influence of atomic-scale disorder increases. For example, one defect per thousand atoms in a conventional metal barely affects conductivity, but in a carbon nanotube the same defect concentration can mean the difference between a metallic and a semiconducting state [1]. Many reduced-dimensional or quantum electronic (RD/QE) devices exhibit unusual sensitivity to disorder. Examples include low- and high temperature superconductors (LTS and HTS), resonant tunneling diodes and resonant interband tunneling diodes (RTDs and RITDs), high electron mobility transistors (HEMTs), and superlattice (SL) and multiquantum well (MQW) devices for photonic applications.

The systems considered here are AlAs/InGaAs/InAs/InGaAs/AlAs RTDs, InAs/AlSb/GaSb/AlSb/InAs RITDs; HEMTs fabricated from GaAs/AlGaAs, InGaAs/AlGaAs, InGaAs/InGaP, and InGaAs/InAlAs; MQW infrared (IR) detectors fabricated from GaAs/AlGaAs and InGaAs/InAlAs; IR detectors fabricated from InAs/GaSb superlattices; and LTS and HTS materials. In these systems, either transport occurs in reduced dimension in real- or momentum-space, or transport is expressed by quantum mechanics or ballistic motion rather than by classical mechanics or diffusion. For example, carriers in HEMTs move in a two-dimensional electron gas (2DEG); and resonant transport in RTDs is limited to a 2-D surface in momentum space.

To study disorder effects in these and other systems, it is convenient to use particle irradiation. The production of atomic displacements depends on the rate at which an incident ion loses energy to displacement damage, called the nonionizing energy loss, S. The resulting defect concentration c is often expressed in units of displacements per target-material atom, or dpa. For relatively small particle fluences Φ, the defect concentration is [2,3]

$$c = \Phi\, S\, B\, A \;, \qquad (1)$$

where B depends on the target material density and the displacement energy threshold of target atoms, and A represents the fraction of displaced atoms that do not recombine immediately following irradiation. For example, as calculated using the Monte Carlo program SRIM [4], the nonionizing energy loss of 3-MeV He^+ ions in a $YBa_2Cu_3O_{7-\delta}$ thin film is about 0.32 $MeV \cdot cm^2/g$. At a fluence of 4×10^{13} He^+/cm^2, the defect concentration before recombination is on the order of 10^{-4} dpa.

In the above example, He^+ ions traverse the film without significant energy loss, creating a uniform damage profile (mainly point defects) across the sample. The same holds true for all particles and devices considered here. Below, we present data on disorder effects in various RD/QE systems, and explain the results in terms of the interaction between disorder, quantum transport, and reduced dimension.

1 SUPERCONDUCTORS

Radiation damage studies on LTS have been done using isotropic metals (like Nb and Pb), A-15 compounds (like Nb_3Sn and Mo_3Si), and other phases [5-7]. Comparable studies on HTS have been done for many HTS systems, including $YBa_2Cu_3O_{7-\delta}$ and $Tl_2Ba_2CaCu_2O_8$ [8-10]. For the present purposes, the parameter of interest here is the transition temperature, T_c. Figure 1 shows the rate of decrease of T_c with Φ, $|dT_c/d\Phi|$, for many HTS and LTS materials, plotted versus S for various incident ions [5-10]. On average, T_c in LTS metals is 10-100 times less sensitive to disorder than in LTS A-15 compounds, which are in turn 10-100 times less sensitive than HTS. For LTS metals and A-15s, the data are widely scattered, but for HTS the data are strongly correlated around the line

$$dT_c/d\Phi = w\, S \;, \qquad (2)$$

where $w = 5 \times 10^{-21}$ $g \cdot K/eV^2$ regardless of incident ion, material, or onset T_c.

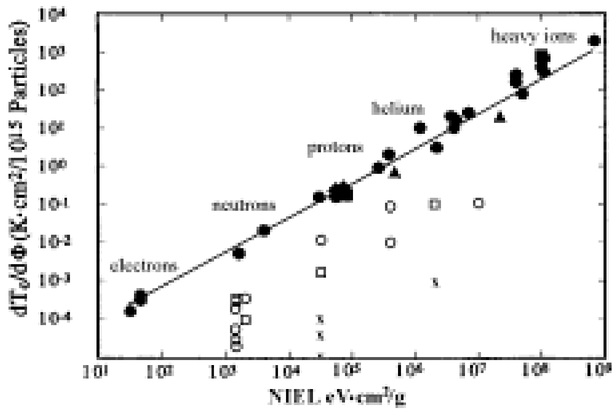

FIGURE 1. Rate of decrease of T_c with Φ vs. nonionizing energy loss (NIEL) for HTS materials (solid symbols), LTS A-15 compounds (open symbols) and LTS metals (x's). Line is Eq. (2) in text.

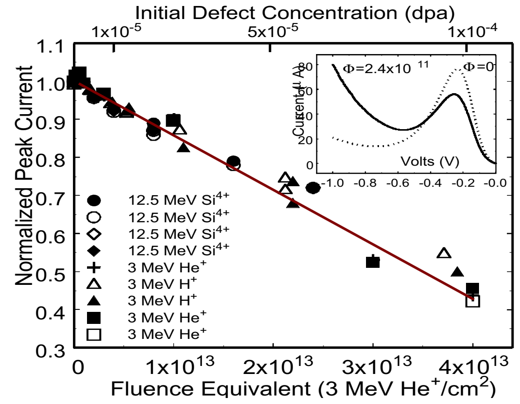

FIGURE 2. Normalized I_p vs. Φ for RTDs. I_p decreases linearly with Φ for all arrays. Inset: IV curves before and after irradiation with 12.5-MeV Si^{4+} ions.

Equations (1) and (2) can be used to show that the reduction in T_c in HTS is directly proportional to the induced defect concentration. The strong resistance of LTS metals to radiation damage was explained by Anderson [11]. In LTS, current is carried by electron pairs whose momentum and spin obey the pairing condition ($\mathbf{k}\uparrow$, $-\mathbf{k}\downarrow$). When electron pairs scatter from elastic, nonmagnetic defects (as are most radiation-induced defects), the direction of each electron changes, but pairing is not broken. As a result, defects barely alter the superconducting state, and quantum mechanics grants isotropic superconductors a strong immunity to disorder.

A-15 compounds are more sensitive to radiation damage than LTS metals because they are not truly isotropic. HTS cuprates are more sensitive still, since superconductivity in HTS is confined to 2-D Cu-O planes, and the pairing condition is compressed into the parallel direction ($\mathbf{k}_{||}\uparrow$, $-\mathbf{k}_{||}\downarrow$). Because defects on Cu-O planes scatter paired electrons into three dimensions, defects remove carriers from the planes and from the superconducting state with high efficiency [9]. The observed reduction in T_c occurs regardless of material properties, and gives rise to the strongly-correlated data for HTS in Fig. 1. Thus, it is the reduced dimensional aspect of superconductivity in HTS that increases the sensitivity of T_c to disorder.

3 TUNNEL DIODES

Because RTDs contain a quantum well between two barriers, only those electrons whose momenta lie on a narrow disk in k-space can undergo resonant tunneling from source to drain. The RTD structure studied here is AlAs/InGaAs/InAs/InGaAs/AlAs [12]. For testing purposes, devices were wired into arrays containing 100 or 1000 RTDs in parallel, then irradiated with either 3-MeV He^+ ions, 3-MeV H^+, or 12.5-MeV Si^{4+}. The parameter of interest here, determined from the current-voltage (IV) curves, is the current at the tunneling transmission peak, I_p.

IV curves for a typical RTD are shown in the inset of Fig. 2 for an irradiated and unirradiated device. The peak in the curve is due to resonant tunneling at about −0.2 V. In the main body of Fig. 2, the normalized peak current $I_p(\Phi)/I_p(0)$ is plotted vs. equivalent 3-Mev He^+ ion fluence for all twelve arrays tested, and for the three different ions used. (To convert 3-MeV H^+ and 12.5-MeV Si^{4+} fluences to equivalent He^+ fluences, scaling factors of 0.052 and 87 were used to compensate for differences in nonionizing energy loss [13]). The striking result is that I_p decreases linearly with Φ, and thus with defect concentration, regardless of the cross-sectional area of devices, the incident particle mass or energy, or the number of diodes in an array. With c expressed in dpa,

$$I_p(\Phi)/I_p(0) \approx 1 - 5500\,c \quad . \tag{3}$$

It is no coincidence that Eq. (3) for the fluence dependence of I_p in RTDs has the same form as that for T_c in irradiated HTS. When defects are introduced into an RTD by irradiation, scattering increases throughout the device. But because RTDs are majority carrier devices, scattering that occurs outside the quantum wells alters the transport current only slightly by decreasing mobility. Inside the well, however, where the electron density of states is 2-D, scattering from defects easily removes carriers from the transport current by ejecting them from the resonance disk. It has been shown that for narrow resonances and reasonably small values of c in irradiated RTDs, a linear relationship between I_p and the defect concentration follows from an expression for the scattering probability [14].

Unlike in RTDs, tunneling in RITDs requires carrier transitions between valence and conduction bands. These transitions require interactions with phonons or other lattice excitations, which effectively broaden the resonance disk in k-space and render it not strictly 2-D. The RITDs considered here contained a pair of nominally

identical AlSb barriers sandwiching a 27 monolayer (ML) GaSb well. A description of the devices and samples of IV curves are given elsewhere [15]. The striking result is that irradiation causes the peak current to increase slightly. This increase is due to increased leakage current through nonresonance channels, and lower out-scattering of carriers due to the broader (i.e., non-2-D) resonance in k-space as compared to RTDs [15].

4 HEMTS

Schematically, HEMTs consist of a source and drain separated by a gate region in which transport occurs by conduction through a 2DEG [16]. Typically, the 2DEG region exists within the upper layer of a low bandgap channel material adjacent to a doped higher bandgap barrier material. For example in GaAs/AlGaAs HEMTs, a higher-bandgap doped AlGaAs layer injects carriers into a 2DEG in the upper part of the undoped GaAs. The current that reaches the drain, I_d, depends in part on the applied voltages, the carrier concentrations, mobilities and lifetimes in the 2DEG.

Values of I_d for different Φ were collected for a variety of HEMTs, incident ions and ion energies, then normalized by the drain current at zero fluence, I_{do}. Values of $\Delta(I_d/I_{do})/\Delta\Phi$ were then calculated and plotted versus nonionizing energy loss. Results are shown in Fig. 3, where it can be seen that the data for GaAs/AlGaAs and InGaAs/AlGaAs HEMTs fall on the line

$$\Delta(I_d/I_{do})/\Delta\Phi = - d\, S \quad , \qquad (4)$$

where $d = 5 \times 10^{-18}$ g/eV. Variations in $\Delta(I_d/I_{do})/\Delta\Phi$ due to different gate lengths, driving voltages etc. are visible as small deviations of the data from the line. The implication of Eq. (4) is that I_d in irradiated (In)GaAs/AlGaAs HEMTs decreases in direct proportion to the induced defect concentration. The same conclusion can be drawn for InGaAs/InGaP HEMTs, except that $d = 3 \times 10^{-19}$ g/eV. In other words, InGaAs/InGaP HEMTs are about 17 times more rad-tolerant than (In)GaAs/AlGaAs HEMTs. Furthermore, InGaAs/InAlAs HEMTs are about 30 times more rad-tolerant than (In)GaAs/AlGaAs HEMTs. From Fig. 4, it can be deduced that rad-tolerance in HEMTs is determined by the barrier material rather than in the 2DEG.

As is the case in RTDs and HTS, scattering of carriers from defects in the reduced-dimensional channels in HEMTs removes carriers from the transport current with high efficiency. Taken alone, this phenomenon would cause I_d to decrease linearly in Φ with the same slope for all HEMTs. Clearly from Fig. 4, this is not the case. Unlike in RTDs and HTS, electrons scattered out of a 2DEG in a HEMT do not necessarily remain out. Due to a higher conduction band edge in the barrier, it is energetically favorable for scattered carriers to be reinjected into the 2DEG. The linear decrease of I_d with Φ arises from high-efficiency scattering *out* of the 2DEG, but the slope is determined by the reinjection rate, which depends on the barrier material via the energy difference between barrier and channel. [17]

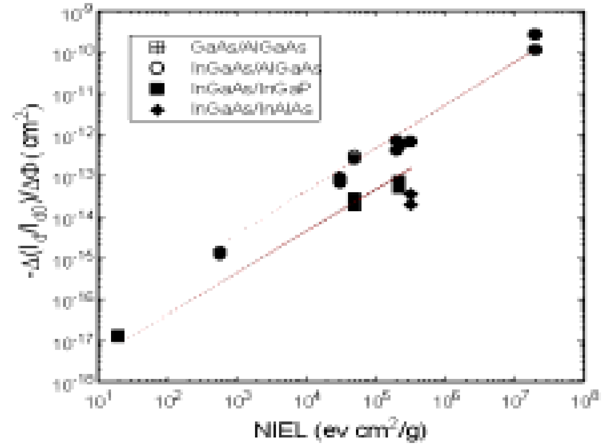

FIGURE 3. Radiation-induced change in drain current vs. nonionizing energy loss in various irradiated HEMTs. Lines are from Eq. (4) in text.

5 MQWS AND SUPERLATTICES

In MQW IR detectors (also known as quantum well infrared photodetectors or QWIPs) bound states in quantum wells trap electrons in 2DEGs, where carriers can absorb incident photons and transition into conduction bands. We studied the effect of radiation damage on the peak absorbance A_{max} in the IR spectrum of intersubband transitions at 77 K in two QWIP systems: GaAs/AlGaAs MQWs irradiated with 3-MeV He^+ ions, and InGaAs/InAlAs MQWs irradiated with 1-MeV protons. (1-MeV protons are about 5.3 times less damaging than 3-MeV He^+ ions.) Details on device geometry are presented elsewhere [18,19].

For the GaAs/AlGaAs QWIPs, a fluence of 1×10^{13} 3-MeV He^+/cm^2 reduced A_{max} to 75% of its original value. By interpolation from the data [18], one would expect a decrease in A_{max} of only about 3% for the same defect concentration in InGaAs/InAlAs QWIPs. (Decreases in A_{max} are thought to be due to defect-induced trapping of carriers in the 2DEG rather than by scattering of carriers out of the 2DEG [18].) It appears that InGaAs/InAlAs QWIPs are, like InGaAs/InAlAs HEMTs, more radiation-tolerant than their GaAs/AlGaAs counterparts. The reason for this behavior currently unknown.

Antimonide superlattice IR photodiodes (ASLs) differ from QWIPs in two main ways. First, they rely on optical transitions between unbound states derived from

superlattice minibands, and second, the transition is interband between valence and conduction subbands. For these reasons ASL's can simulate a real semiconductor with a direct (in k-space) IR gap adjustable from 3 to > 20 μm. Most importantly, unlike QWIP structures, ASLs are suitable for implementation of minority carrier based photodetection, resulting in lower thermally-generated noise than majority carrier devices. The binary ASLs discussed here had periods composed of 13 ML of InAs on 13 ML of GaSb and having a 7.3-μm cutoff wavelength [20]. Devices were exposed to incremental fluences of 1-MeV H^+ ions. A fluence of $10^{13}/cm^{-2}$ resulted in about one order of magnitude degradation in R_0A**,** the dynamic impedance at zero bias scaled by area, which is a key photodiode figure of merit reflecting dark current performance. Though the detailed mechanisms of degradation are not yet known, it appears that ASL diodes, like other minority carrier devices, are more sensitive to radiation-induced disorder than their majority carrier counterparts.

CONCLUSIONS

We conclude with a comparison of radiation tolerance in various conventional and RD/QE devices. For each device, a parameter of merit (e.g. T_c, I_d, A_{max}) was chosen, and the equivalent fluence of 3-MeV He^+ ions was estimated for causing a 5% change in the parameter. The results, shown in Fig. 4, reveal ten orders of magnitude of variation in radiation-tolerance. LTS leads the way, due to the quantum mechanical immunity granted as a result of electron pairing. High-T_c superconductors share a similar but lesser immunity due to their reduced dimensional nature. Below HTS in Fig. 4 are classical majority carrier devices such as plain resistors, followed by reduced-dimensional or quasi-reduced-dimensional majority carrier devices such as RTDs, RITDs, HEMTs and QWIPs. Below these are the minority carrier devices.

It is clear from Fig. 4 that quantum mechanics and reduced dimension have a strong effect on how electronic devices respond to disorder. As the state of the art continues to advance, we expect many more intersting discoveries to be made involving the effects of disorder in RD/QE systems.

This research was supported in part by the Office of Naval Research, DTRA and AFOSR.

REFERENCES

[1] L. Chico, V.H. Crespi, L.X. Benedict, S.G. Louie M.L. Cohen, Phys. Rev. Lett. **76**, 971 (1996).
[2] J.F. Kircher and R.E. Bowman, "Effect of Radiation on Materials and Components," Reinhold, 480-508, 1964.
[3] J. Lindhard, V. Nielsen, M. Scharff and P. Thomsen, Mat. Fys. Medd. Dan. Vid. Selsk. **33**, 1 (1963).
[4] J.F. Ziegler, J.P Biersack and U. Littmark, "The Stopping and Range of Ions in Solids," Vol. 1, Pergamon, 1985. (The latest version of SRIM is available on-line at http://www.research.ibm.com/ionbeams.)

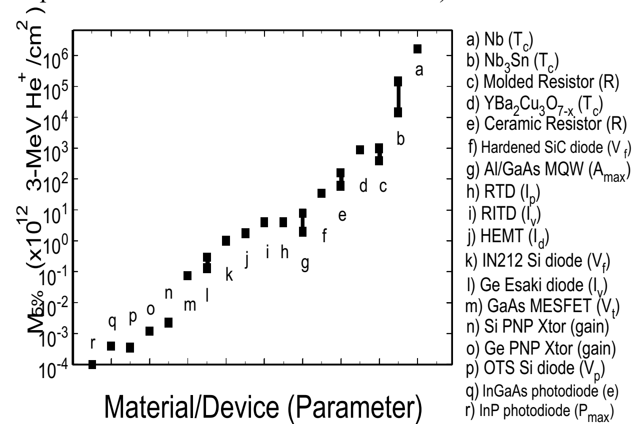

FIGURE 4. Fluence of 3-MeV He^+ required to change operating parameters by 5%. V_f: forward voltage drop. V_t: threshold voltage. e: efficiency of solar cells. P_{max}: maximum power.

[5] B.S. Brown, J.W. Hafstrom and T.E. Klippert, J. Appl. Phys. **48**, 1759 (1977).
[6] A.R. Sweedler, D.G. Schweitzer and G.W. Webb , Phys. Rev. Lett. **33**, 168 (1974).
[7] A.R. Sweedler, D.E. Cox and S. Moehlecke, J. Nucl. Matl. **72**, 50 (1978).
[8] B.D. Weaver, M.E. Reeves, D.B. Chrisey, G.P. Summers, W.L Olson, M.M. Eddy, T.W. James and E.J. Smith, J. Appl. Phys. **69**, 1119 (1991).
[9] B.D. Weaver, E.M. Jackson, G.P. Summers and E.A. Burke, Phys. Rev. B **46**, 1134 (1992).
[10] B.D. Weaver, G.P. Summers, R.L. Greene, E.M. Jackson, S.N. Mao, and W. Jiang, Phys. C **261**, 229 (1996).
[11] P.W. Anderson, J. Phys. Chem. Solids **11**, 26 (1959).
[12] A. Seabaugh and R. Lake, Encycl. Appl. Phys. **22**, 335 (1998).
[13] B.D. Weaver, E.M. Jackson, A.C. Seabaugh P.W. van der Wagt, Appl. Phys. Lett. **76**, 2562 (2000).
[14] B.D. Weaver, E.M. Jackson, G.P. Summers and A.C. Seabaugh, J. Appl. Phys. **88**, 6951 (2000).
[15] R. Magno, B.D. Weaver, A.S. Bracker and B.R. Bennett, Appl. Phys. Lett. **78**, 2581 (2001).
[16] A. Seabaugh, B. Brar, T. Broekaert, F. Morris, P. van der Wagt and G. Frazier, Sol. St. Electon. **43**, 1355 (1999).
[17] B.D. Weaver and E.M. Jackson, submitted to Appl. Phys. Lett., Aug, 2001.
[18] Y. Berhane, M.O. Manasreh and B.D. Weaver, J. Appl. Phys. **89**, 3517 (2001).
[19] J. Chen, Q. Zhou, M.O. Manasreh, B.D. Weaver, and M. Missous, to be publ. in MRS Proceedings (Fall 2001

MRS Meeting, Symposium H, 26-30 November, Boston, MA).
[20] E.H. Aifer and B.D. Weaver, to be submitted to Appl. Phys. Lett.